STUDY OF A RENEWABLE ENERGY POWER PLANT WITH A SOLAR TOWER CHIMNEY AND A FLAT COLLECTOR

DONA Victorien Bruno[1], MAXWELL Djaffard[2], TOVONDRAINY Ramiandrisoa[2]
RATIARISON Adolphe Andriamanga[3]

[1]*Doctor, Department of physics, Laboratory of Applied Physics and Renewable Energies, Mahajanga, University*
[2] *Doctor, Department of physics, Laboratory of Applied Physics and Renewable Energies, Mahajanga, University*
[3] *Emeritus Professor, Department of physics, Laboratory of Atmospheric, Climate and Ocean Dynamics, University of Antananarivo*

ABSTRACT

This article contributes to the modeling and simulation of a solar tower chimney equipped with a horizontal solar collector with a natural thermal storage system, the ground, which is below the collector. The objective is the prediction of the thermal and electrical performance of the plant as well as the study of the influences of the external and internal parameters of the solar chimney tower. This study also shows the possibility of predicting the temperature variation across the collector and the temperature rise from the inlet to the outlet of the collector and the parameters that influence the temperature rise of the solar chimney.

Key words: *Solar chimney, Solar collector, Thermal storage, Energy performance, Thermal balance, Heat exchange coefficients.*

I.INTRODUCTION

Generating a natural movement of air in the form of artificial wind from solar energy, and using this airflow to drive a wind turbine, this combination of two types of solar energy exploitation has become possible using solar chimney technology. The basic idea is that solar radiation could be transformed into another form of energy into heat and electricity from a three-part solar-wind hybrid system: the solar collector or greenhouse, the chimney or tower, and the wind turbine. The main advantage of this technology is that the system can operate without intermittent operation using direct and diffuse solar radiation during the day and heat released from the ground or an additional thermal storage system at night. Even under overcast skies, diffuse radiation can be exploited by the solar tower chimney for power generation. This work meets two objectives, namely: prediction of the energy performance of the solar tower chimney as a function of certain external (solar irradiation and ambient temperature) and internal (physical or geometric parameters: tower height, collector diameter, collector roof height) parameters of the plant. The study focuses on assessing the power that a solar chimney power plant operating under the Mahajanga site weather condition can produce for all months of the year. As well as, estimating the temperature distribution through the collector and the temperature rise from inlet to outlet of the collector.

II. METHODOLOGIES

2.1-Configuration adopted and operating principle

The configuration adopted, shown in Figure 1, is a single-glazed horizontal solar tower chimney power plant equipped with only a natural storage system, the ground (Figure 1). The solar tower chimney works thanks to the combination of several known and controlled physical phenomena: natural convection phenomenon, thermosiphon phenomenon, greenhouse effect, Archimedes' thrust, chimney effect, Venturi effect, Coriolis force and electromagnetic induction phenomenon[1].

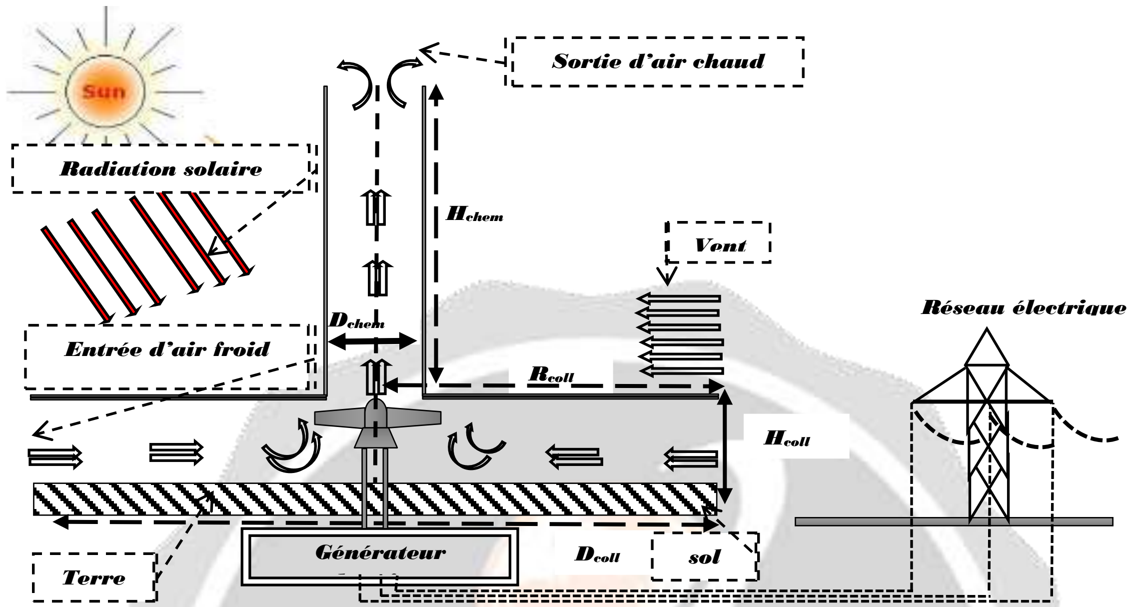

Figure 1: Schematic diagram of the operation of a solar tower chimney plant with upward air movement

The collector is open at the periphery to introduce fresh air that will be heated by the sun's rays, under the greenhouse effect, where the temperature difference between inside and outside produces a gradient in the density of the rising internal air.

A wind turbine positioned at the base of the chimney, in the air flow path, extracts a quantity of available energy from the flowing air (kinetic energy), in the form of rotational mechanical energy and the generator, driven by the turbine, converts the mechanical energy into electrical energy. The chimney converts the thermal energy referred to the collector into kinetic energy and potential energy [2].

2.2-Mathematical modelling

The mathematical formulation of the solar tower chimney plant requires the use of equations from thermodynamics, fluid mechanics and radiation physics. The proposed model depends on the parameters that influence the output power, namely: external parameters: meteorological conditions, which are represented by solar insolation, temperature and wind speed. The internal parameters: the configuration of the solar chimney, represented by the size of the chimney and the solar collector: the height of the chimney, the diameter of the collector radius and the height of the collector periphery [1,2].

2.2.1-Modelling of horizontal global solar irradiation

The Garg model is used to estimate the monthly average per day of the global irradiation on a horizontal plane from the meteorological parameters relating to the site linking the extraterrestrial solar irradiation calculated on a horizontal plane G0, the monthly averages of the insolation fraction, the absolute humidity Ha, the relative humidity HR and the ambient temperature Ta [3].

$$G_H = G_0\left(0,14 - 0,4\left(\frac{S}{S_0}\right) - 0.0055Ha\right) \quad (1)$$

$$Ha = HR\left(4,7923 + 0.347T_a + 0.0055T_a^{\,2} + 0.0003T_a^{\,3}\right)$$

$$G_0 = \frac{24}{\pi} I_{SC}\left[\cos(\varphi)\cos(\delta)\sin(\omega_s) + \omega_s \sin(\varphi)\sin(\delta)\right]$$

At the limit of the atmosphere, the daily insolation is identical to the theoretical insolation So which corresponds to the duration of the day. It depends only on the latitude of the site and the declination.

$$S_0 = \frac{2}{15}\cos^{-1}(-\tan(\varphi)\times\tan(\delta))$$

The monthly mean daily diffuse solar irradiation striking a horizontal plane is expressed as a function of KT ,the fraction of irradiation or monthly mean daily solar brightness index, and is derived from the relationship :

$$\frac{G_d}{G_H} = \begin{cases} 1,311 - 3,022K_T + 3,427K_T^{\,2} - 1,821K_T^{\,3} & \text{pour } 0,3 < K_T \le 0,8 \text{ et } \omega_s > 81,4^\circ \\ 1,391 - 3,560K_T + 4,189K_T^{\,2} - 2,137K_T^{\,3} & \text{pour } 0,3 < K_T < 0,8 \text{ et } \omega_s \le 81,4^\circ \end{cases} ; K_T = \frac{G_H}{G_0}$$

The average daily direct irradiation per month striking a horizontal plane

$$G_D = G_H - G_d \quad (2)$$

The solar irradiations absorbed by the glass solar collector, the absorber and the ground are expressed as follows:

$$G_{coll} = \alpha_{coll}\times\tau_{coll}\times G_H$$
$$G_{sol} = \alpha_{sol}\times\tau_{coll}\times G_H \quad (3)$$

2.2.2. Modelling of the single-glazed solar collector

a) Heat exchange balance

This study is based on the following assumptions [1,2]:
1. The plant's performance is analyzed at steady state, since solar radiation and ambient temperature are transient under real conditions.
2. Air is a perfect gas and the flow rate is incompressible in the chimney because the Mach number is less than 0.3.
3. The air flow in the system is due to the buoyancy force of the solar chimney.
4. The collector is placed on the horizontal surface and the air flow in the collector is considered as a uniform flow between two parallel plates.
5. The heat loss from the sensor is due solely to convection and radiation.
6. The flow in the collector is considered as a flow between two parallel plates

For the modelling of heat exchanges in the solar collector, the slice or step-by-step modelling method is used. It consists in cutting the solar collector into fictitious slices in the direction of the flow of the heat transfer fluid, and using the analogies that exist between the heat transfer and the equivalent analog electrical circuits. The different heat exchanges that take place in the collector and the equivalent electrical circuit for a section of the collector are shown in Figure 2.

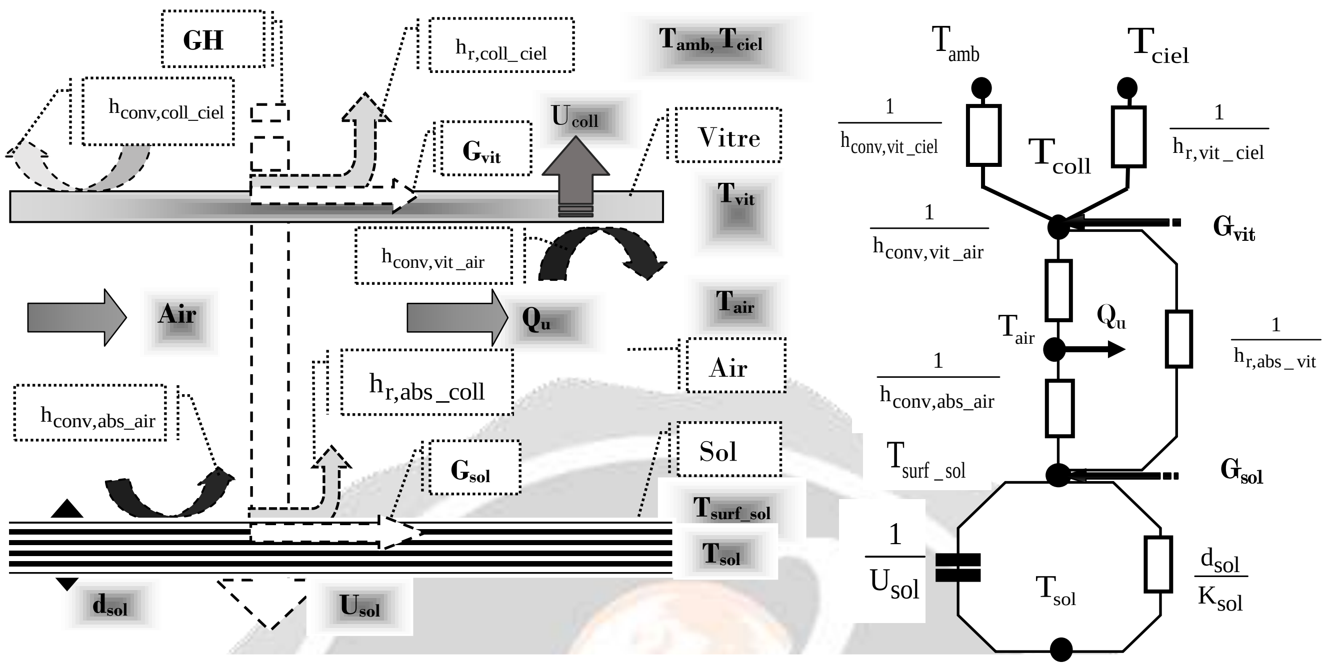

Figure 2: Heat exchange and equivalent electrical network of the single-glazed solar collector

The application of Ohm's law on the equivalent electrical circuit leads to the equations of the heat exchange balances in the different parts of the solar collector [4,5]:

$$\left|\begin{array}{l} Au\ niveau\ de\ vitrage:\ Noeud\ T_{coll} \\ G_{coll}+h_{r,surfsol\_coll}\times\left(T_{abs}-T_{coll}\right)+h_{conv,coll\_air}\times\left(T_{air}-T_{coll}\right)=Q_{pertes\_coll} \\ Au\ niveau\ de\ l'air\ en\ écoulement:\ Noeud\ T_{air} \\ h_{conv,coll\_air}\times\left(T_{coll}-T_{air}\right)+h_{conv,surfsol\_air}\times\left(T_{surfsol}-T_{air}\right)=Q_{air} \\ Au\ niveau\ du\ sol\ (l'absorbeur):\ Noeud\ T_{surfsol} \\ G_{sol}+h_{conv,surfso\_air}\times\left(T_{air}-T_{surfsol}\right)+h_{r,surfsol\_coll}\times\left(T_{coll}-T_{surfsol}\right)=Q_{pertes\_sol} \end{array}\right. \qquad (4)$$

$$\begin{cases} G_{coll}=h_{r,surfsol\_coll}\times\left(T_{coll}-T_{surf\_sol}\right)+h_{conv,coll\_air}\times\left(T_{coll}-T_{air}\right)+U_{coll}\times\left(T_{coll}-T_{amb}\right) \\ h_{conv,coll\_air}\times\left(T_{coll}-T_{air}\right)+h_{conv,surfsol\_air}\times\left(T_{surf\_sol}-T_{air}\right)=\Gamma\left(T_{air}-T_{air\_in}\right) \\ G_{sol}=h_{r,surfsol\_coll}\times\left(T_{surf\_sol}-T_{coll}\right)+h_{conv,surfsol\_air}\times\left(T_{surf\_sol}-T_{air}\right)+U_{sol\_tot}\times\left(T_{surf\_sol}-T_{sol}\right) \end{cases} \qquad (5)$$

The equation system (5) can be rewritten as a matrix equation of dimension (3x3) as follows[4,5]:

$$\begin{bmatrix} h_{r,abs\_coll}+h_{conv,coll\_air}+U_{coll} & -h_{conv,coll\_air} & -h_{r,abs\_coll} \\ h_{conv,coll\_air} & -\left(h_{conv,coll\_air}+h_{conv,abs\_air}+\Gamma\right) & h_{conv,abs\_air} \\ -h_{r,abs\_coll} & h_{conv,abs\_air} & -\left(h_{r,abs\_coll}+h_{conv,abs\_air}+U_{sol\_tot}\right) \end{bmatrix}\begin{bmatrix} T_{coll} \\ T_{air} \\ T_{abs} \end{bmatrix}=\begin{bmatrix} G_1+U_{coll}T_{amb} \\ -\Gamma T_{air\_e} \\ -\left(G_2+U_{sol\_tot}T_{sol}\right) \end{bmatrix} \qquad (6)$$

Either in a general form:

$$\begin{bmatrix} a_{11} & a_{12} & a_{13} \\ a_{21} & a_{22} & a_{23} \\ a_{31} & a_{32} & a_{33} \end{bmatrix} \begin{bmatrix} T_{coll} \\ T_{air} \\ T_{abs} \end{bmatrix} = \begin{bmatrix} b_1 \\ b_2 \\ b_3 \end{bmatrix}$$

Temperatures are determined by matrix inversion.

$$[\mathrm{T}] = [\mathrm{B}] \times [\mathrm{A}]^{-1} \qquad (7)$$

The resulting matrix is solved iteratively, and the newly calculated temperatures are compared with the previous values until they converge. The convergence tolerance is defined so that the difference between the new temperature and the estimated temperature is less than 0.01 K.

The useful heat transferred to the moving air stream is determined by considering the temperature distribution along the direction of air flow in a section of the collector, as shown in Figure 3.

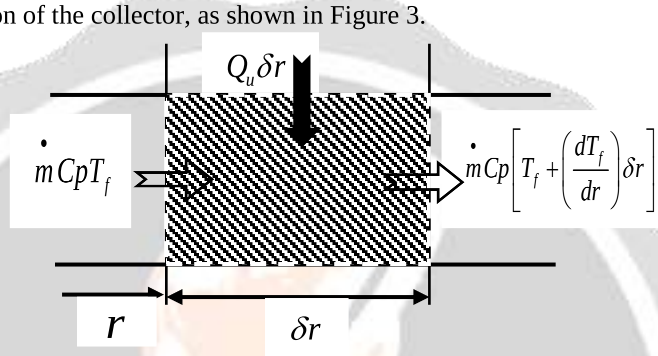

Figure 3: Thermal exchanges in a fictitious collector slice

The energy conservation in this section of the length sensor L gives[1,2]:

$$\dot{m} C p T_f + Q_u 2\pi r dr = \dot{m} C p \left(T_f + \frac{dT_f}{dr} \delta r \right) \qquad (8)$$

After simplification, and taking into account the assumptions: the air temperature can be assumed to be uniform throughout the fluid layer of the length sensor L and it varies in a linear manner over each section of the collector, the average temperature is equal to the arithmetic mean. The integration of energy balance leads to the following equation:

$$T_{air} = \frac{T_{air,ent} + T_{air,sort}}{2}, T_{air,sort} - T_{air,ent} = \frac{Q_{air} 2\pi r H_{coll}}{\dot{m}_{air} C p_{air}} \qquad (9)$$

The net heat flux transmitted to the flowing air can be defined in relation to the average fluid temperature and the inlet temperature, as follows:

$$Q_{air} = \frac{\dot{m}_{air} C p_{air}}{\pi r H_{coll}} \left(T_{air} - T_{air,in} \right) = \Gamma \left(T_{air} - T_{air,in} \right), \ \Gamma = \frac{\dot{m}_{air} C p_{air}}{\pi r H_{coll}}; \quad r = D_{coll} / 2 \qquad (10)$$

b) Modeling of thermal transfer coefficients

-Coefficient of thermal transfer by radiation between the glazing and the sky

$$\mathrm{h}_{\mathrm{r,coll\_ciel}} = \frac{\sigma \varepsilon_{\mathrm{coll}} \left[\left(\mathrm{T_{coll}} + \mathrm{T_{ciel}} \right) \left(\mathrm{T_{coll}^2} + \mathrm{T_{ciel}^2} \right) \left(\mathrm{T_{coll}} - \mathrm{T_{ciel}} \right) \right]}{\left(\mathrm{T_{coll}} - \mathrm{T_{amb}} \right)} \qquad (11)$$

$$\mathrm{T_{ciel}} = 0{,}0552.\mathrm{T_{amb}^{\frac{3}{2}}} \qquad (12)$$

-Convection transfer coefficient between glass and ambient air

$$h_{cv,coll\_amb} = h_{vent} = 5.67 + 3.86.V_{vent} \tag{13}$$

-Coefficient of heat transfer by radiation between the glass and the absorber (the floor)

$$h_{r,abs\_coll} = \frac{\sigma\left(T_{coll} + T_{abs}\right)\left(T_{coll}^2 + T_{abs}^2\right)}{\left[\frac{1}{\varepsilon_{coll}} + \frac{1}{\varepsilon_{abs}} - 1\right]} \tag{14}$$

-Coefficient of heat exchange by convection between the collector and the air flow and between the air flow and the ground.].

$$h_{conv,coll\_air} = h_{conv,abs\_air} = N_u \frac{k_{air}}{d_h} \tag{15}$$

The collector is circular with a radius of rcoll and height of Hcoll, hydraulic diameter:

$$d_h = \frac{4 \times A_{coll}}{P_{coll}} = \frac{4\left(2\pi r_{coll} H_{coll}\right)}{2\left(2\pi r_{coll} + H_{coll}\right)} \cong 2H_{coll}$$

The Nusselt number for horizontal sensors, for natural convection in laminar mode is given as follows:

$$\begin{cases} N_u = 0,76 \times Ra^{0,25} \text{ pour } \quad 10^4 < Ra < 10^7 \\ N_u = 0,15 \times Ra^{0,6} \text{ pour } \quad 10^7 < Ra < 10^{10} \end{cases}$$

The Rayleigh number Ra is defined as the product of the numbers Grashof Gr and Prandtl Pr and is equal to :

$$Ra = Gr \times Pr, \quad Gr = \frac{g\beta\left(T_{abs} - T_f\right)H_{coll}^3}{\upsilon^2} \quad \text{et} \quad Pr = \frac{\upsilon}{\alpha}$$

The coefficient of volumetric thermal expansion is given as follows:

$$\beta = \left[0,25T_{amb} + 0,75T_f\right]^{-1}$$

c) Modeling of heat loss coefficients

-Overall heat loss coefficient of the collector

The overall heat loss coefficients are the combination of all heat losses from the collector surfaces: heat losses from the upper glass surface, the lower surface and the edges. Assuming that the heat losses from the bottom surface and edges are negligible, the overall heat loss coefficient of the collector is written:

$$U_{coll} = \frac{1}{R_{th,vit\_amb} + R_{th,sol\_vit}} \tag{16}$$

The thermal resistance between the glass cover and the ambient air / sky is mainly due to the forced convection of the wind and the exchange of radiation with the sky. The equivalent thermal resistance between the ground and the collector glass is mainly due to natural convection inside the collector and radiation between the two surfaces.

$$R_{th,vit\_amb} = \frac{1}{h_{conv,vit\_amb} + h_{r,vit\_ciel}} \quad ; \quad R_{th,sol\_vit} = \frac{1}{h_{conv,sol\_vit} + h_{r,vit\_sol}}$$

-Overall heat loss coefficient of the absorbing soil

The total heat loss from the ground is expressed as a function of the heat transfer coefficient to the ground, the thermal conductivity of the ground k_{sol}, the depth of temperature variation d_{sol} [6]:

$$U_{sol\_tot}=\frac{1}{\frac{1}{U_{sol}}+\frac{d_{sol}}{k_{sol}}}\ ;\ U_{sol}=2\sqrt{\frac{k_{sol}\rho_{sol}Cp_{sol}}{\pi t}}\ ;\quad d_{sol}=\sqrt{\frac{2\alpha}{\omega}};\omega=\frac{2\pi}{t} \qquad (17)$$

In this model, an average value for a period t of 84600 seconds is used in the calculation of the energy in one day and T_{sol} is equal to T_{amb}. α is the thermal diffusivity of the ground, ω is the daily angular frequency which is equal to 0.0000727s-1. t is the time from midnight [6].

(d) Thermal efficiency of the collector

The collector efficiency can be expressed as a function of the estimated useful energy required to produce hot air in the collector, as follows[1.6]:

$$\eta_{coll}=\frac{Q_u}{A_{coll}G_{coll}} \qquad (18)$$

According to Duffie and Beckman, based on the energy balance equation for the
solar collector, it follows that the useful energy is the difference between the optical energy produced by the solar collector and the energy lost in the solar collector:

$$Q_u=Q_{opt}-Q_{perd};\ Q_{opt}=F_RA_{coll}G_{coll}\ ;\ Q_{perd}=F_RA_{coll}U_{coll}\left(T_{surf\_sol}-T_{amb}\right) \qquad (19)$$

2.2.4-Stack Modelling

Stack modeling consists of modelling the total air pressure difference between the base and top of the stack, the stack performance.

a-Total pressure difference inside the chimney

If friction losses are negligible, the total pressure difference between the base and top of the chimney is the sum of the static pressure difference which represents the pressure drop through the turbine, and the dynamic pressure difference which describes the kinetic energy of the air. The approximation of the dynamic pressure difference required to accelerate the air through the stack using the Bernoulli equation gives[4,5,6]:

$$\Delta p_{dyn}=\frac{1}{2}\rho_{air,chem}V_{air,chem}^2 \qquad (20)$$

The static pressure drop at the turbine is determined as follows:

$$\Delta p_{stat}=\Delta p_{tot}-\frac{1}{2}\rho_{air,chem}V_{air,chem}^2 \qquad (21)$$

In case the system is not coupled with a turbine, the entire pressure difference is used to accelerate the air (converted into kinetic energy), a maximum air velocity Vchem, max is reached. Thus the total power contained in the air flow is given by:

$$\Delta p_{tot}=\frac{1}{2}\rho_{air,chem}V_{air,max}^2 \qquad (22)$$

b-Air flow velocity in the chimney

In the absence of a turbine, the maximum air velocity in the stack[1,4,5]:

$$V_{air,max}=\sqrt{\frac{2\Delta p_{tot}}{\rho_{air}}} \qquad (23)$$

As a result, the actual wind speed in the stack, when a turbine is installed, is one-third of the maximum air speed in the stack in the absence of a turbine:

$$V_{air}=\frac{1}{3}\sqrt{\frac{2\Delta p_{tot}}{\rho_{air}}} \qquad (24)$$

Due to buoyancy, the total pressure difference is determined as follows:

$$\Delta p_{tot} = \rho_{air} g\left(H_{chem} + H_{coll} / 2\right) \quad (25)$$

It comes, the expression of the actual velocity of the air flow in the chimney:

$$V_{air} = \frac{1}{3}\sqrt{2g\left(H_{chem} + \frac{H_{coll}}{2}\right)} \quad (26)$$

c-Check chimney performance

The efficiency of the chimney is expressed by the ratio of the power contained in the flow and the solar power relative to the next collector:

$$\eta_{che} = \frac{P_{tot}}{Q} = \frac{g \times H_{chem}}{Cp \times T_0} \quad (27)$$

2.2.5- Air turbine modeling

The useful power at the output of the turbine and the generator is the power absorbed by the turbine which is given by the relationship :

$$P_{U,turb} = \Delta p_{stat} \times A_{chem} \times V_{air,chem} \quad (28)$$

The maximum power is achieved when the pressure drop in the turbine is equal to two thirds of the total pressure difference available:

$$\Delta p_{stat} = \frac{2}{3}\Delta p_{tot} \quad (29)$$

$$P_{elect} = P_{turb,max} = \frac{2}{3}\Delta p_{tot} \times A_{chem} \times V_{air,chem} \quad (30)$$

III. RESULTS AND DISCUSSIONS

3.1-Characteristics of the Mahajanga site

The geographical location of the Mahajanga site is defined in Table 1.

Table 1: Mahajanga site geographical coordinates

Locality	Latitude Φ	Longitude L	Altitude A	Reference meridian LST	Albedo of the ground as
Mahajanga	15,40' Sud	46,21° Est	22 m	40°	0,35

3.2-Temporal variations in solar irradiation and electrical power produced by the stack

The curves in Figure 1 show the evolution of the solar radiation received on a horizontal plane as well as the evolution of the power delivered by a solar power plant with a chimney on a typical day for the months of October and December of the year 2017. It is clear from the curves that the solar power is at its maximum between 12:00 and 14:00. The overall monthly irradiation varies according to the months considered, it is maximum, in the order of 966 Wh.m-2, in October and minimum, with a value of 609 Wh.m-2, in December.

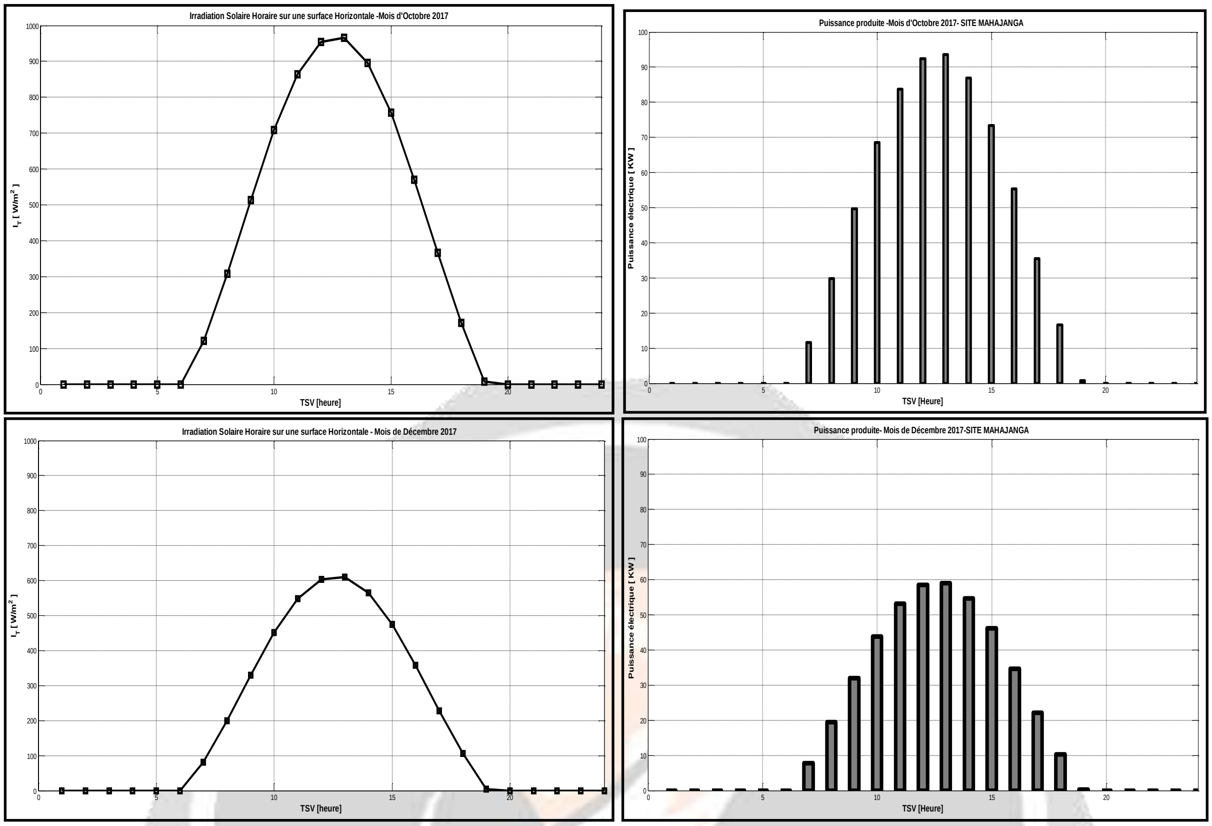

Figure 1: Instantaneous variations in horizontal solar irradiation received and electrical power in October and December 2017 - Mahajanga site

October is therefore the most favourable month and well adapted to the applications and exploitation of solar energy. The irradiance is all the more important during the period from May to November, during which the potential of solar energy varies between 823 and 966W.m-2.

As for the instantaneous evolution of the power generated by solar installations, it is of the same nature as that of solar radiation. The minimum value is obtained during months when the solar radiation rate is low and the maximum value is obtained during the period corresponding to the month when the solar energy potential is highest. The power of the electrical energy developed is also important during the months when the solar radiation rate is at its highest, it is around 95 kW, for the installation with the ground as storage system.

3.3-Temporal variation of absorbed powers

The curves of variation with time, for the months of October and December, of the absorbed powers of the glass and the absorber are presented in Figure 2. The absorbed powers follow the same law as the temporal variation of the global radiation because these powers are linked to the global radiation by linear laws. The solar power absorbed by the absorber is important because of its high absorption coefficient, unlike the transparent cover which has a very low absorbed power, this is due to its optical properties, namely its low absorption coefficient and its high transmission coefficient.

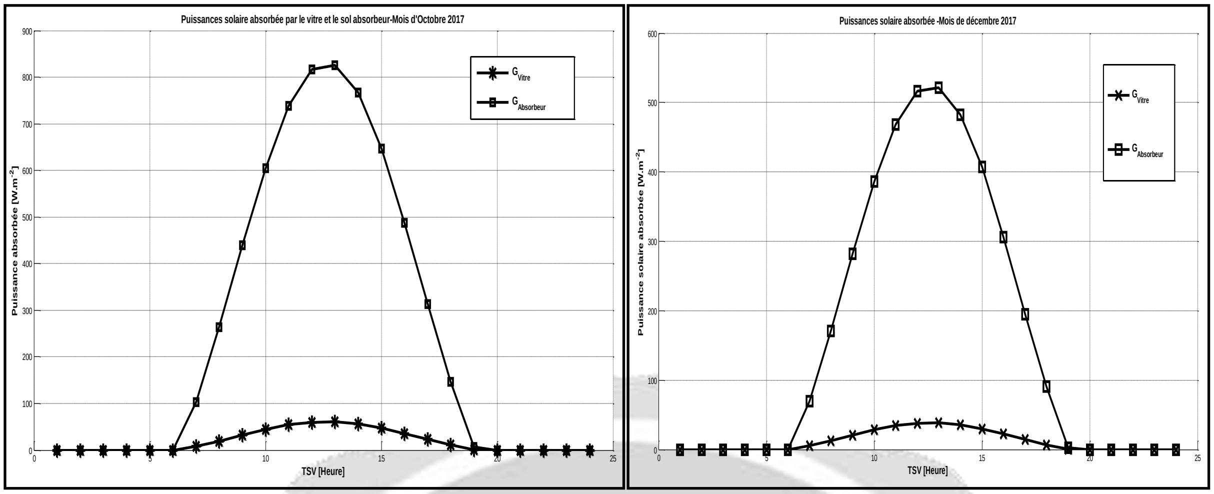

Figure 2: Solar power absorbed by the glass and the absorber

3.4-Temporal changes in ambient and sky temperatures

According to Figure 3, The temperature of the sky varies according to that of the atmosphere, it follows that the curves representing the temporal evolution of the temperatures of the atmosphere and the sky have the same appearance, they reach their maximum values between 13h00 and 15h00 as well as the global radiation, this is explained by the greenhouse effect.

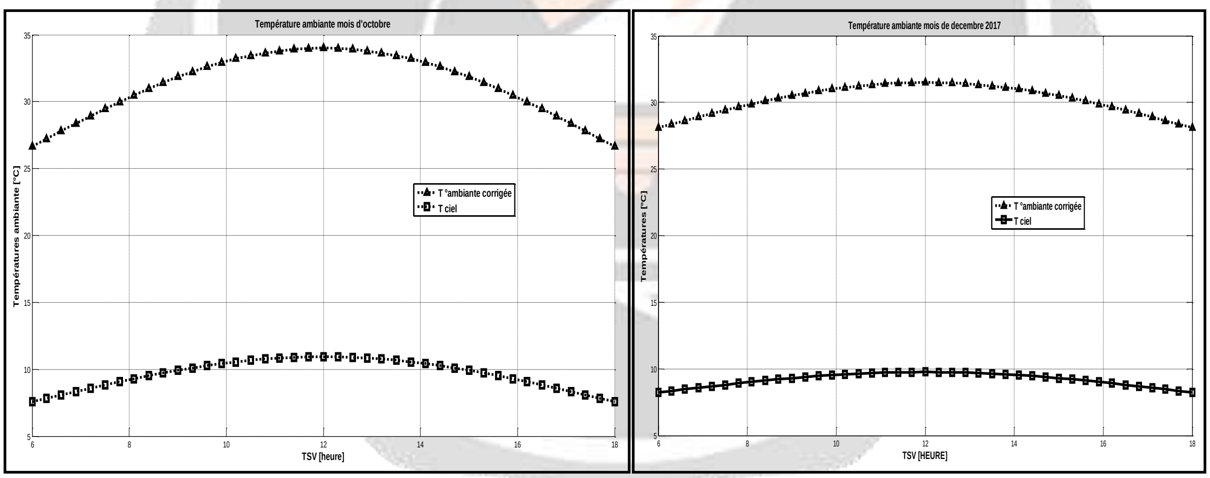

Figure 6: Temporal variation in ambient and sky temperatures for the months of October and December 2017

3.5-Temporal variation of the temperatures of the different parts of the sensor

According to Figure 7, the different temperatures of the solar collector components vary proportionally with the power absorbed by each component and reach their maximum values in the period 12h-14h.

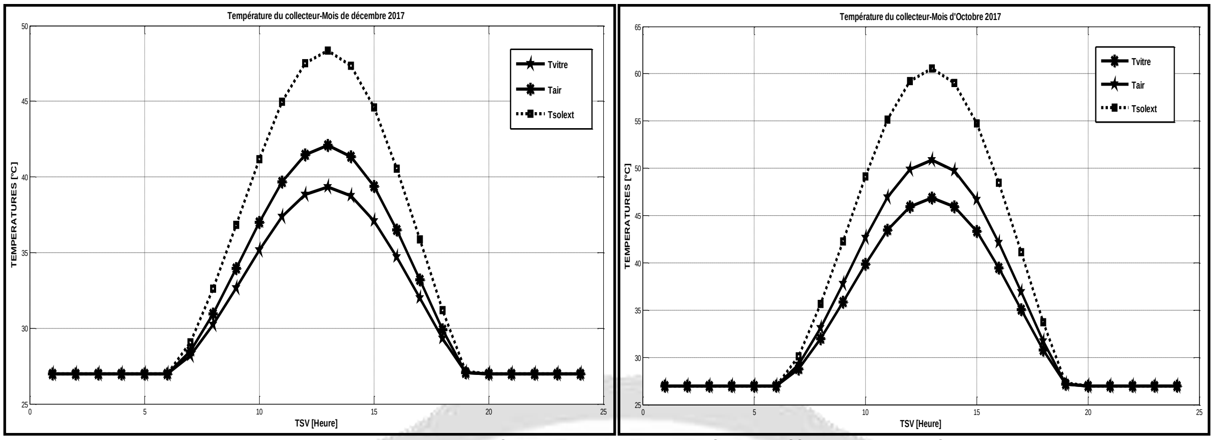

Figure 7: Time evolution of the temperatures of the different parts of the solar collector during the months of October and December-Site Mahajanga

The highest temperature is that of the absorber (the ground), resulting from the high solar power it has absorbed. The glass temperature is the lowest because transparent glass has a low absorption coefficient and transmits a large part of the solar energy to the absorber. The air temperature between the glass and the floor is slightly higher than that of the glass, which is explained by the absorption of incident radiation on the one hand, and the heat released by the absorber in the form of radiation and convection on the other.

3.6-Influence of mass flow on the temperature of the coolant air

Figure 8 shows the hourly evolution of the coolant air temperature for several mass flow values for the two months of October and December. The amount of energy transferred depends mainly on the thermo-physical characteristics of the fluid and in particular on its flow rate. When the input flow rate is lowest, the heat transfer rate is higher. The air flow rate increases with increasing solar radiation, and the distance between the absorber and the glass increases. Thus for the month of October, the air temperature under the collector reaches a value of 51°C with a mass flow equal to 0.01 kg.s-1 while in December, the temperature value is 42.3°C for the same mass flow.

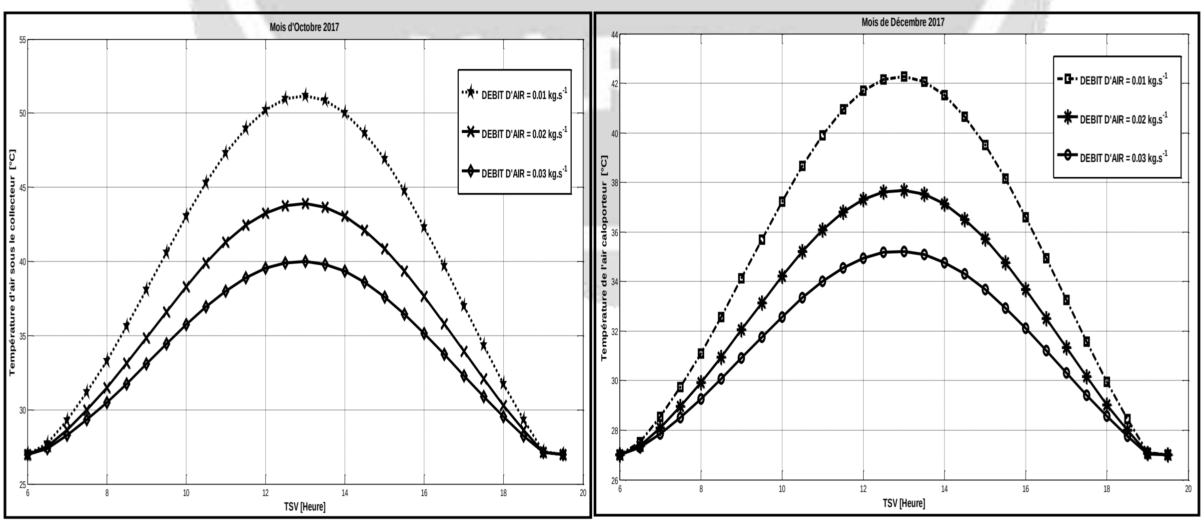

Figure 8: Effect of mass flow on coolant air temperature

IV.CONCLUSIONS

The results obtained in this study show that the Mahajanga region has the favourable weather conditions to operate a solar chimney tower plant continuously throughout the day. However, electricity production is relatively linked to the rates of solar radiation, which varies according to the month of the year. The power of the solar chimney increases with the increase in solar flux, which will cause the temperature of the absorber to increase, affecting the air temperature. An increase in solar flux causes an increase in absorber and glazing temperatures and the average air temperature below the collector, and its decrease also causes their decrease. The increase in chimney height is used to increase the air velocity at the chimney inlet. The increase in stack diameter allows for an increase in mass flo Given the importance of this topic for the future, this study will serve as a basis for further more detailed work and will lead to the construction of a scale model prototype and an industrial prototype in Madagascar.

V.REFERENCES

[1]- Mr. SEMAI Hakim, Research for an optimal configuration of a solar chimney power plant, Doctoral thesis in Energy Physics, Abu-Bekr Belkaid University - Tlemcen, 2017.
M. DENIS BONNELLE, Solar tower, water vaporization tower, and related renewable energy conversion modes: presentation, criticisms and suggestions, thesis of the Claude Bernard University - Lyon 1 - France, 2004.
[3] -H.P. Garg and S.N. Garg,'Prediction of Global Solar Radiation from Bright Sunshine Hours and Other Meteorological Data', Energy Conversion and Management, Vol. 23, N°2, pp. 113 - 118, 1983.
[4] T. Chergui, S. Larbi, A. Bouhdjar Thermo-hydrodynamic aspect analysis of flows in solar chimney power plants - A case study. Renewable and Sustainable Energy Reviews. (2010)
[5] Chergui T., M. Lebbi, Abd. H. Boualit, L. Boutina, A. Bouhdjar, S. Larbi. Analysis of the effect of Ambient Temperature on the Thermo-hydrodynamic field of Solar Chimneys.19-21-December.2014-CIER 2014. In Monastir, Tunisia.
[6] Mohammed H. Ali, Analysis Study of Solar Tower Power Plant & Its Configuration Effects on Its Performance in Iraq (Baghdad City), Modern Applied Science; Vol. 7, No. 4; 2013w, which is reflected in the increase in productivity in proportion to the diameter of the stack.